On the Rheology of Newtonian Single-Phase Multicomponent Mixtures

Sverre Gullikstad Johnsen[1,2]

[1]SINTEF Industry, Trondheim, Norway
[2]NTNU, dept. Materials Science and Engineering, Trondheim, Norway

ABSTRACT

In the turbulent boundary layer of multicomponent fluid mixtures, the species-specific mass flux is determined by the combination of turbulent-diffusiophoretic diffusion and diffusion due to gradients in supplementary fields (e.g. temperature). For inert mixtures, a balance must exist between all the diffusive transport mechanisms so that the net diffusive mass flux normal to the wall is zero everywhere. This may require non-constant composition profiles.

Implications are discussed, and mathematical modelling is employed to demonstrate how this may affect fluid property profiles, wall heat flux, and wall shear stress in a Newtonian ternary gas mixture ($H_2 + N_2 + CO_2$) subject to a temperature gradient.

INTRODUCTION

In their classical experiment, Duncan and Toor[4] showed that the diffusive transport in an ideal ternary gas mixture of hydrogen (H_2), nitrogen (N_2), and carbon dioxide (CO_2) could not be described satisfactorily by the Fickian formulation. E.g., the observed development in local nitrogen concentrations could only be explained mathematically by allowing uphill diffusion. The Duncan-Toor experiments have been further investigated and discussed by e.g. Taylor and Krishna[11] and Krishna and Wesselingh.[9] It has been shown that Maxwell-Stefan diffusion predicts the non-Fickian behavior observed by Duncan and Toor, accurately.

Whereas the Duncan-Toor experiments were performed under isothermal conditions, Bogatyrev et al.[3] studied thermophoresis in binary, ternary, and quaternary mixtures including the ternary $H_2 - N_2 - CO_2$ mixture. They emphasized that thermophoresis in multicomponent mixtures depends on the mixture composition in a complex way.

In this paper, it is hypothesized that non-Fickian behavior can cause non-constant composition profiles in the turbulent boundary layer of inert mixtures. Zero net transport for each species is required, in the direction normal to the wall, but it is suggested that competing diffusive processes (e.g. turbulent, diffusiophoretic and thermophoretic diffusion) which cancel each other out can occur. This implies that non-constant mass-fraction profiles may be necessary to give zero net diffusive transport.

The concern is that these spatial composition variations will affect fluid properties (e.g. mass density, viscosity, heat capacity, and thermal conductivity) hence the wall heat flux and wall shear stress. Thus, without the proper understanding, interpretation of rheology measurements may fail to give a correct assessment of the fluid properties, even for relatively simple Newtonian ideal mixtures.

Using the ideal ternary gas mixture of Duncan and Toor[4] as an example, mathematical modelling of the species transport in the fully developed turbulent boundary layer is employed to support the hypothesis. Comparing simulations with and without diffusion, it is demonstrated that a significant effect on wall heat flux and wall shear stress can be expected from the diffusion-induced non-constant composition profiles.

MATHEMATICAL MODELS

We are considering a single-phase fluid mixture consisting of a set of N unique, distinguishable, inert species. It is assumed that each species

field, hence the fluid itself, can be modeled as a continuum. This implies that species properties are well defined, continuously varying physical fields throughout the fluid domain. Furthermore, it is assumed homogeneous mixing in the sense that local species properties are taken as volume averages over infinitesimal volumes. These assumptions allow the utilization of differential calculus in deriving governing equations for the species transport.

Governing Equations

The set of steady-state governing equations consists of the Advection-Diffusion equation (ADE) for each species,

$$\boldsymbol{\nabla}\left(\rho_f X_i \boldsymbol{u}_f\right) + \boldsymbol{\nabla}\boldsymbol{j}_{d,i} = 0\,, \tag{1}$$

the fluid mixture momentum and energy equations,

$$\boldsymbol{\nabla}\left(\rho_f \boldsymbol{u}_f \boldsymbol{u}_f\right) = -\boldsymbol{\nabla}P + \boldsymbol{\nabla}\boldsymbol{\tau} + \rho_f \boldsymbol{g}\,, \tag{2}$$

$$\boldsymbol{\nabla}\left(\rho_f h_{sens,f} \boldsymbol{u}_f\right) = \boldsymbol{\nabla}\left(k_f \boldsymbol{\nabla}T\right) - \boldsymbol{\nabla}\left(\sum_{i=1}^{N} \boldsymbol{j}_{d,i} h_{sens,i}\right)\,, \tag{3}$$

and the restriction that the mass- and mole-fractions must sum to unity,

$$\sum_{i=1}^{N} X_i = \sum_{i=1}^{N} z_i = 1\,. \tag{4}$$

Introducing turbulence, dimensionless variables (see Appendix) and appropriate simplifications, the simplified governing equations are obtained:

$$\left(v_t^+ \rho_f^+ / Sc_t\right) \partial_\perp X_i - j_{d,i,\perp}^+ = 0\,, \tag{5}$$

gives the mass-fraction profiles;

$$\partial_\perp u_{f,\parallel}^+ = {}^1/\left(\mu^+ + \mu_t^+\right)\,, \tag{6}$$

gives the dimensionless axial fluid mixture velocity profile; and

$$\partial_\perp \left[k_t^+ \left(\partial_\perp \ln c_P^+\right) T^+ + \left(k_f^+ + k_t^+\right) \partial_\perp T^+\right] = 0\,, \tag{7}$$

gives the dimensionless temperature profile. The $\perp$ and $\parallel$ indicate the directions normal to and parallel with the wall and the bulk flow direction, respectively, and $\partial_\perp$ denotes the dimensionless gradient component in the direction perpendicular to the wall. Fore more details, refer to Johnsen *et al.*[7]

Diffusion flux

Employing Maxwell-Stefan theory,[11] the dimensionless diffusive mass flux of species i normal to the wall can be expressed as

$$j_{d,i,\perp}^+ = -\rho_f^+ D_{ij}^+ \partial_\perp \mu_j \tag{8}$$

$$= -\rho_f^+ D_{ij}^+ \left[\Gamma_{jk}\Lambda_{kl}\partial_\perp X_l + d_{\psi,j}\partial_\perp \psi\right]\,, \tag{9}$$

where Einstein summation is employed, and the diffusive driving force consists of two terms; namely a diffusiophoretic term due to composition gradients, and a phoretic term due to gradients in other scalar fields (e.g. temperature). The D_{ij} are the multicomponent diffusion coefficients, $\Gamma_{jk} = {}^{\partial_{z_k}\mu_j}/_{RT}$, $\Lambda_{kl}\partial_\perp X_l = \partial_\perp z_k$, $d_{\psi,j} = {}^{\partial_\psi \mu_j}/_{RT}$. The chemical potential of species j is expressed as $\mu_j = \mu_j^0 + \mu_j^\psi + RT\ln\left(\gamma_j z_j\right)$, where μ_j^ψ represents the potential contribution from the supplementary, scalar fields. In the presence of a temperature gradient, the supplementary field gradient can be written

$$d_{\psi,j}\partial_\perp \psi = \left({}^{\partial_T \mu_j}/_R\right) \partial_\perp \ln\left(T^+ + T_{wall}^{0+}\right)\,. \tag{10}$$

It follows from the definitions, that the diffusive mass flux of the Nth, dependent species is given by $j_{d,N,\perp}^+ = -\sum_{i=1}^{N-1} j_{d,i,\perp}^+$. Hence it suffices to solve Eqs. (5)-(7) for $i \in \{1,\ldots,N-1\}$.

Combining Eqs. (5) and (8), it is seen that zero net mass transport can only be ensured by requiring that

$$D_{ij}^+ \partial_\perp \mu_j = -\left(v_t^+ / Sc_t\right) \partial_\perp X_i\,. \tag{11}$$

In the following two paragraphs, the implications of this requirement is investigated for two scenarios: 1) the absence of supplementary field gradients ($\partial_\perp \psi = 0$); and 2) the presence of a temperature gradient ($\partial_\perp \psi = \partial_\perp \ln\left(T^+ + T_{wall}^{0+}\right)$).

Turbulent-Diffusiophoretic Diffusion

In the case of $d_{\psi,j}\partial_\perp \psi = 0$, Eq. (5) can be written as the homogeneous system of equations

$$\mathcal{D}^+_{X,il}\partial_\perp X_l = 0 \,, \tag{12}$$

where $\mathcal{D}^+_{X,il} = \left[\left(\nu_t^+/Sc_t\right)\delta_{il} + D^+_{ij}\Gamma_{jk}\Lambda_{kl}\right]$, and δ_{il} is the Kronecker delta. It is readily shown that Eq. (12) has a non-trivial solution ($\partial_\perp X_l \neq 0$) if and only if $-\nu_t^+/Sc_t$ is an eigenvalue of the matrix product $\boldsymbol{D}^+\boldsymbol{\Gamma}\boldsymbol{\Lambda}$.

At the wall, where $\nu_t^+/Sc_t \to 0$, the required condition for non-trivial solution reduces to $\det(\boldsymbol{\Gamma}) = 0$, since both $\boldsymbol{D}^+$ and $\boldsymbol{\Lambda}$ are invertible. For ideal mixtures, $\gamma_j = 1$ for all j, so

$$\Gamma_{jk,\text{ideal}} = \delta_{jk}/z_j \,. \tag{13}$$

Hence, ideal mixtures permit the trivial solution ($\partial_\perp X_l = 0$) only, at the wall, absent supplementary field gradients.

Combined Turbulent-Diffusiophoretic and Thermophoretic Diffusion

In the presence of thermophoresis (due to temperature gradients), there must be a balance between the turbulent-diffusiophoretic diffusion on one side and thermophoretic diffusion on the other. This can be expressed as the nonhomogeneous system of equations

$$\mathcal{D}^+_{X,il}\partial_\perp X_l = -\mathcal{D}^+_{T,i}\partial_\perp \ln\left(T^+ + T^{0+}_{wall}\right) \,, \tag{14}$$

where $\mathcal{D}^+_{T,i} = D^+_{ij}d_{T,j}$. It is evident that nonzero mass-fraction gradients are required to counter the thermophoresis, in general.

At the wall, Eq. (14) reduces to

$$\Gamma_{jk}\partial_\perp z_k\big|_{wall} = -d_{T,j,wall}Pr_{wall}/T^{0+}_{wall} \,. \tag{15}$$

For ideal mixtures, Eqs. (4) and (15) require that $\sum_{j=1}^{N} z_j d_{T,j} = 0$ holds at the wall. This implies that d_Ts of both positive and negative values must exist at the wall, for ideal mixtures.

MODEL FLUID

The model fluid is a ternary, calorically perfect mixture of perfect gasses consisting of 50, 25, and 25 mass-% of H_2, N_2, and CO_2, respectively. Species specific heat capacities were extracted from the NIST Chemistry WebBook[1] while species specific viscosities and thermal conductivities were calculated based on Lennard-Jones parameters found in Andersson.[2] Details regarding the modelling of species and mixture material properties (mass density, viscosity, etc.) can be found in Johnsen et al.[7] Species specific input data are summarized in Table (1).

Table 1. Species specific properties.

			Lennard-Jones param.	
	M_w [kg/mol]	c_P^1 [J/molK]	d [Å]	Ω^1 [−]
H_2	0.002016	28.84	2.915	0.857
N_2	0.02801	29.12	3.681	1.022
CO_2	0.04401	37.12	3.996	1.296

[1] values at 298K.

For a ternary mixture, there are two independent mass-fraction equations in addition to the velocity and temperature equations. Moreover, there are only two independent diffusive mass-fluxes, and the matrices that take part in Eq. (9) are 2×2 matrices.

The elements of the diffusivity matrix, $\boldsymbol{D}$, can be expressed as[11]

$$\begin{aligned} D_{11} &= Đ_{13}\left[z_1 Đ_{23} + (1-z_1)Đ_{12}\right]/S \,, \\ D_{12} &= z_1 Đ_{23}\left[Đ_{13} - Đ_{12}\right]/S \,, \\ D_{21} &= z_2 Đ_{13}\left[Đ_{23} - Đ_{12}\right]/S \,, \\ D_{22} &= Đ_{23}\left[z_2 Đ_{13} + (1-z_2)Đ_{12}\right]/S \,, \end{aligned} \tag{16}$$

where $S = z_1 Đ_{23} + z_2 Đ_{13} + z_3 Đ_{12}$, the $Đ_{ij}$ are the binary Maxwell-Stefan diffusion coefficients, and 1, 2 and 3 relate to H_2, N_2, and CO_2, respectively. The binary Maxwell-Stefan diffusivities employed by Duncan and Toor[4] are cited in Table (2). It is noted that the Onsager reciprocal relation implies that $Đ_{ij} = Đ_{ji}$.[5,10]

Bogatyrev et al.[3] reported thermal diffusion factors, α_T, as functions of composition for each of the mixture species. The thermal diffusion factors are related to the diffuiophoretic driving force, $d_{T,j}$ via the thermal diffusion ratio, $k_{T,k}$, by[12]

$$d_{T,j} = \Gamma_{jk}k_{T,k} \,, \tag{17}$$

Table 2. Binary Maxwell-Stefan diffusion coefficients for the ternary $H_2 - N_2 - CO_2$ mixture.[4]

$H_2 - N_2$	$Đ_{12} = 8.33 \cdot 10^{-5} \mathrm{m^2/s}$
$H_2 - CO_2$	$Đ_{13} = 6.80 \cdot 10^{-5} \mathrm{m^2/s}$
$N_2 - CO_2$	$Đ_{23} = 1.68 \cdot 10^{-5} \mathrm{m^2/s}$

where

$$k_{T,k} = z_k \sum_{\substack{l=1 \\ l \neq k}}^{N} z_l \alpha_{T,kl} \ . \tag{18}$$

For ideal mixtures, Eq. (17) reduces to

$$d_{T,j} = \sum_{\substack{l=1 \\ l \neq j}}^{N} z_l \alpha_{T,jl} \ . \tag{19}$$

Using the experimental data points at $z_l \approx 0.5$ from Bogatyrev et al.,[3] the thermal diffusion factors and thermophoretic driving force coefficients given in Table (3) were obtained. For simplicity, constant $d_{T,j}$ were employed in the simulations.

Table 3. Thermal diffusion factors, $\alpha_{T,jl}$, based on data from Bogatyrev et al.[3] and resulting thermophoretic driving force coefficients, $d_{T,j}$ (assuming ideal mixture, see Eq. (19)).

j	α_{T,j,H_2}	α_{T,j,N_2}	α_{T,j,CO_2}	$d_{T,j}$
H_2		0.32	0.38	0.161
N_2	0.24		0.06	0.073

SIMULATION SETUP

The equations were solved in a numerical modelling framework described by Johnsen et al.[7] The simulations assume fully developed turbulent flow parallel to the wall. Moreover, it is assumed that gradients in the main flow direction are negligible and that gradients perpendicular to the wall vanish in the bulk. Additional details can be found in Johnsen et al.[7]

The wall and bulk temperatures were set equal to the Bogatyrev et al.[3] temperatures of $280K$ and $800K$, respectively, and a range of bulk flow velocities were employed. The boundary conditions employed in the simulations are summarized in Table (4).

The simulations were conducted on a 1-dimensional computational mesh consisting of 30 grid points logarithmically distributed between the wall and the bulk. A grid sensitivity study showed that the wall heat flux and wall shear stress varied with less than 1% between a grid with 30 grid points and one with 100 grid points. The first grid point was located 10^{-7}m away from the wall, and the bulk node was located 10^{-3}m away from the wall. The results were insensitive to decreasing the first node distance to the wall.

To isolate the effect of non-zero composition gradients, simulations with and without diffusion were conducted. In the simulations without diffusion, the multicomponent diffusion coefficients were zero, $D_{ij} = 0 \ \forall \ i, j$.

Table 4. Boundary Conditions employed in simulations.

Boundary Condition	**Variable**	**Value**	**Unit**
bulk mass-fractions	$X_{H_2,bulk}$	0.5	$\mathrm{kg/kg}$
	$X_{N_2,bulk}$	0.25	$\mathrm{kg/kg}$
wall diffusion mass flux	$j_{d,H_2,\perp,wall}$	0	$\mathrm{kg/m^2s}$
	$j_{d,N_2,\perp,wall}$	0	$\mathrm{kg/m^2s}$
bulk temperature	T_{bulk}	800	K
wall temperature	T_{wall}	280	K
bulk flow velocity	$u_{x,bulk}$	1,2,5,10	$\mathrm{m/s}$

SIMULATION RESULTS

Simulations were performed with and without diffusion. In the simulations without diffusion, the mass-fraction profiles were constant throughout the boundary layer, and fluid properties varied only due to the varying temperature. In simulations including diffusion, however, non-constant mass-fraction profiles resulted to balance the thermophoretic diffusion by turbulent-diffusiophoretic diffusion, to maintain zero net diffusive transport. The resulting mass-fraction profiles are shown in Fig. (1), for the various bulk flow velocities (darker curve corresponds to higher velocity). Generally, the mass-fraction of CO_2 increased towards the wall while H_2 and N_2 mass-fractions

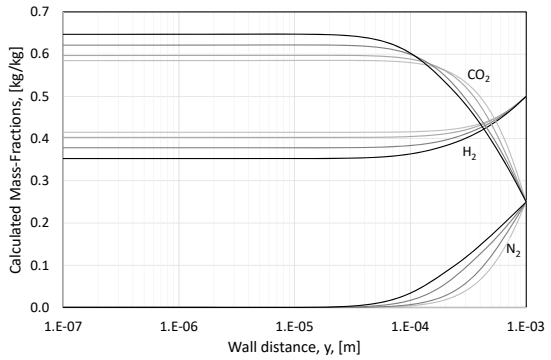

Figure 1. Calculated mass-fractions plotted against wall distance, for the three species H_2, N_2, and CO_2, for the bulk flow velocities 1 (light grey), 2, 5, and 10$^{\mathrm{m}}/_{\mathrm{s}}$ (black).

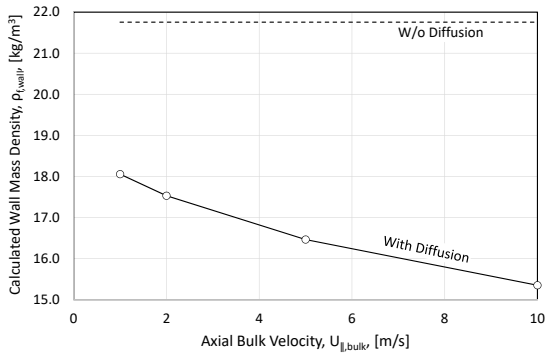

Figure 2. Calculated wall mass density, $\rho_{f,wall}$, plotted against bulk flow velocity.

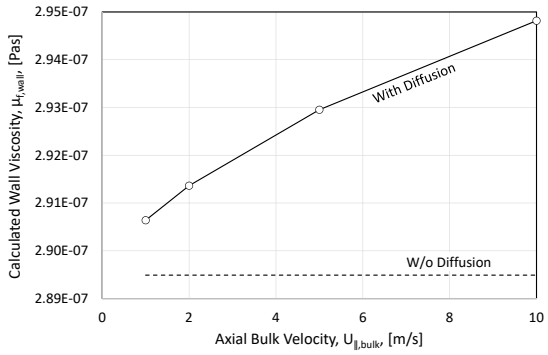

Figure 3. Calculated wall viscosity, $\mu_{f,wall}$, plotted against bulk flow velocity.

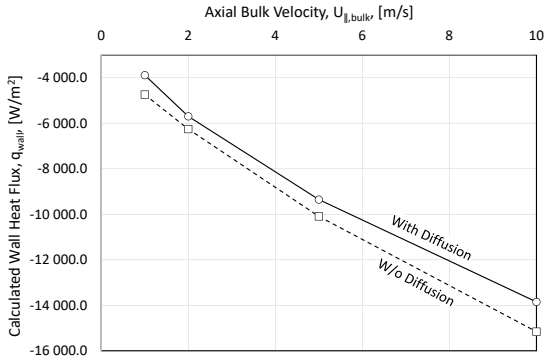

Figure 4. Calculated wall heat flux, q_{wall}, plotted against bulk flow velocity (negative heat flux indicates that heat is flowing from the fluid into the wall).

decreased. Due to the composition dependency in fluid properties (e.g. mass density and viscosity), the simulations predict a bulk flow velocity dependency in these.

In Figs. (2) and (3), respectively, the wall mass density and viscosity are shown as functions of the bulk flow velocity. It is seen that the effect of diffusion is to reduce the mass density and increase the viscosity. In the absence of diffusion, the mass density and viscosity are insensitive to the flow velocity since the wall temperature was fixed.

In Fig. (4), the wall heat fluxes are shown as functions of bulk flow velocity, for simulations with and without diffusion. Negative heat flux indicates that the heat flows from the fluid into the wall, and the magnitude of the heat flux generally increases with the bulk flow velocity, as expected. The simulations predict that diffusion will reduce the efficiency of the heat exchange between the bulk and wall.

In Fig. (5), the wall shear stresses are shown as functions of the bulk flow velocity, for simulations with and without diffusion. The wall shear stress increases with increasing flow velocity, as expected, but the simulations predict that diffusion will reduce the growth rate.

CONCLUSION

Employing mathematical modelling, it has been shown that the combined turbulent, diffusiophoretic and thermophoretic diffusion can have a siginficant effect on composition profiles in the turbulent boundary-layer for in-

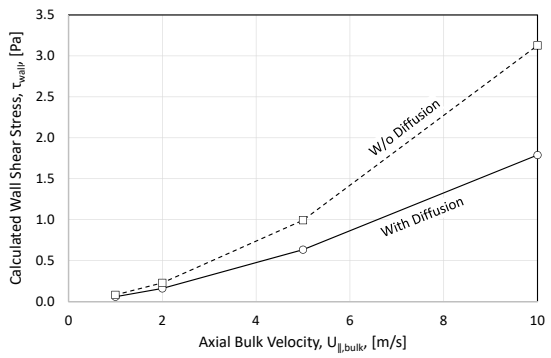

Figure 5. Calculated wall shear stress, τ_{wall}, plotted against bulk flow velocity.

ert, multicomponent fluids. This is of importance for the interpretation of rheology measurements to establish e.g. viscosity and thermal conductivity, since the fluid composition at the wall may differ significantly from the bulk composition.

Mathematical proof was given to support the following statements for inert mixtures:

- In the absence of supplementary scalar field gradients:
  - Non-constant composition profiles requires that $-\nu_t/Sc_t$ is an eigenvalue of the matrix product $\boldsymbol{D\Gamma\Lambda}$.
  - Non-zero compositional gradients at the wall requires that $\det(\boldsymbol{\Gamma}) = 0$.
  - Ideal mixture are not permitted to have non-zero compositional gradients at the wall.
- In the presence of a temperature gradient:
  - Non-zero compositional gradients are required to counter the thermophoresis.
  - For ideal mixtures, the thermophoretic driving force coefficients must obey $\sum_{j=1}^{N} z_j d_{T,j} = 0$.

ACKNOWLEDGEMENTS

Gratitude goes to all the colleagues at the research group of flow technology at dept. Process technology, SINTEF Industry, in Trondheim, Norway. Without the vibrant research environment and fruitful discussions, this paper would not be.

NOMENCLATURE

∂_ζ	Partial derivative w.r.t. the arbitrary variable ζ, $1/[\zeta]$.
$\boldsymbol{\nabla}$	The vector differential operator, $1/\mathrm{m}$.
α_T	Thermal diffusion factor, dimensionless.
γ	Activity coefficient, dimensionless.
$\boldsymbol{\Gamma}$	Matrix of diffusiophoretic driving force coefficients, dimensionless.
Γ_{jk}	Element of $\boldsymbol{\Gamma}$, dimensionless.
c_P	Fluid specific heat capacity, $\mathrm{J/kgK}$.
δ_{kl}	Kronecker delta, element of $\boldsymbol{I}$, dimensionless.
$\boldsymbol{d}$	Diffusive driving force vector, $1/\mathrm{m}$.
d_T	Thermophoretic driving force coefficient, dimensionless.
d_ψ	Phoretic driving force coefficient pertaining to the potential energy field ψ, $1/[\psi]$.
$Đ_{ij}$	Binary Maxwell-Stefan diffusion coefficients of species i in species j, $\mathrm{m^2/s}$.
$\boldsymbol{D}$	Matrix of multicomponent diffusion coefficients, $\mathrm{m^2/s}$.
D_{ij}	Element of $\boldsymbol{D}$, diffusivity of species i in species j, $\mathrm{m^2/s}$.
$\boldsymbol{\mathcal{D}}_T$	Column vector of thermophoretic diffusivities, $\mathrm{m^2/s}$.
$\mathcal{D}_{T,i}$	Element of $\boldsymbol{\mathcal{D}}_T$, $\mathrm{m^2/s}$.
$\boldsymbol{\mathcal{D}}_X$	Matrix of turbulent-diffusiophoretic diffusivities, $= (\nu_t/Sc_t)\,\boldsymbol{I} + \boldsymbol{D\Gamma\Lambda}$, $\mathrm{m^2/s}$.
$\mathcal{D}_{X,il}$	Element of $\boldsymbol{\mathcal{D}}_X$, $\mathrm{m^2/s}$.
g	Acceleration, $\mathrm{m/s^2}$.
h_{sens}	Specific sensible enthalpy, $\mathrm{J/kg}$.
$\boldsymbol{I}$	Identity matrix, dimensionless.
$\boldsymbol{j}_d$	Diffusive mass flux vector, $\mathrm{kg/m^2s}$.
k	Thermal conductivity, $\mathrm{Wm/K}$.
k_T	Thermal diffusion ratio, dimensionless.
$\boldsymbol{\Lambda}$	Mass-mole transformation matrix, dimensionless.
Λ_{kl}	Element of $\boldsymbol{\Lambda}$, dimensionless.
μ	Molar chemical potential, $\mathrm{J/mol}$, or dynamic viscosity, Pas.
M_w	Molar mass, $\mathrm{kg/mol}$.
ν	Kinematic viscosity, $\mathrm{m^2/s}$.
N	Number of species in mixture.
P	Pressure, Pa.

Pr	Prandtl number, dimensionless.
ρ	Mass density/concentration, kg/m^3.
R	Universal gas constant, $8.3144598\,\mathrm{J}/\mathrm{Kmol}$.
Sc	Schmidt number, dimensionless.
T	Absolute temperature, K.
$\boldsymbol{\tau}$	Shear-stress tensor, Pa.
$\boldsymbol{u}_f$	Mass-averaged advective fluid velocity vector, m/s.
X	Mass fraction, kg/kg.
y	Distance to the wall, m.
z	Mole fraction, $\mathrm{mol}/\mathrm{mol}$.
ψ	Supplementary potential field, dimensions in accordance with potential field.

Sub/superscripts

$+$	Dimensionless variable.
0	Reference state or value.
$\perp$	Wall-normal component.
f	Property of the fluid mixture.
i,j,k,l	Species indexing.
ψ	Property pertaining to the potential energy field, ψ.
t	Turbulent.
T	Property pertaining to the temperature field.
wall	Value at the wall.

REFERENCES

1. NIST chemistry webbook - NIST standard reference database number 69. https://webbook.nist.gov/chemistry/, 2018.

2. J. D., Jr. Anderson. *Hypersonic and High Temperature Gas Dynamics*. AIAA, 2006.

3. A. F. Bogatyrev, O. A. Makeenkova, and M. A. Nezovitina. Experimental study of thermal diffusion in multicomponent gaseous systems. *International Journal of Thermophysics*, 36(4):633–647, 2015.

4. J. B. Duncan and H. L. Toor. An experimental study of three component gas diffusion. *AIChE Journal*, 8, 1962.

5. J. O. Hirschfelder, C. F. Curtiss, and R. B. Bird. *Molecular Theory Of Gases And Liquids*. Wiley, 1964.

6. S. T. Johansen. The deposition of particles on vertical walls. *International Journal of Multiphase Flow*, 17(3):355–376, 1991.

7. S. G. Johnsen, S. T. Johansen, and B. Wittgens. A wall-function approach for direct precipitation/crystallization fouling in cfd modelling. In *Heat Exchanger Fouling and Cleaning XI - 2015*, 2015.

8. W.M. Kays and M.E. Crawford. *Convective Heat and Mass Transfer*. McGraw-Hill, Inc., 1993.

9. R. Krishna and J.A. Wesselingh. The maxwell-stefan approach to mass transfer. *Chemical Engineering Science*, 52(6):861 – 911, 1997.

10. C. Muckenfuss. Stefan-maxwell relations for multicomponent diffusion and the chapman-enskog solution of the boltzmann equations. *The Journal of Chemical Physics*, 59, 1973.

11. R. Taylor and R. Krishna. *Multicomponent Mass Transfer*. John Wiley & Sons, Inc., 1993.

12. F. Van Der Valk. Thermal diffusion in ternary mixtures: I. theory. *Physica*, 29(5):417 – 426, 1963.

APPENDIX - DIMENSIONLESS VARIABLES

The model equations presented in this paper are presented in dimensionless form. Dimensionless variables are denoted by superscript $+$. When making the conservation equations dimensionless, typical wall unit scaling is employed. Selected scaled variables are given below.

The shear velocity is defined as

$$u_\tau = \sqrt{\tau_w/\rho_{f,wall}} \ , \tag{20}$$

the dimensionless wall distance is defined as

$$y^+ = {}^{yu_\tau}/_{\nu_{f,wall}} \ , \tag{21}$$

where y is the normal distance to the wall. $\nu_{f,wall} = \mu_{f,wall}/\rho_{f,wall}$ is the kinematic viscosity at the wall, the dimensionless fluid velocity is defined as

$$u_f^+ = {}^{u_f}/_{u_\tau} \ , \tag{22}$$

and the dimensionless mass flux is given by

$$j^+ = {}^{j}/_{\rho_{f,wall} u_\tau} \ . \tag{23}$$

Fluid properties are typically converted to wall units by scaling with the value at the wall; e.g.

$$\rho_f^+ = \rho_f/\rho_{f,wall} \ , \tag{24}$$

$$\mu_f^+ = \mu_f/\mu_{f,wall} \ , \tag{25}$$

$$k_f^+ = {}^{k_f}/_{k_{f,wall}} \ . \tag{26}$$

The dimensionless, turbulent thermal conductivity is defined as

$$k_t^+ = \nu_t^+ \rho_f^+ c_P^+ \left({}^{Pr_{wall}}/_{Pr_t}\right) \ , \tag{27}$$

and the dimensionless, turbulent kinematic viscosity is modelled as[6]

$$\nu_{t,f}^+ = \begin{cases} \left({}^{y^+}/_{11.15}\right)^3 & \text{for } y^+ < 3.0, \\ \left({}^{y^+}/_{11.4}\right)^2 - 0.049774 & \text{for } 3.0 \leq y^+ \leq 52.108, \\ 0.4y^+ & \text{for } 52.108 < y^+. \end{cases} \tag{28}$$

Diffusivities are scaled by the fluid kinematic viscosity at the wall, e.g.

$$D_{ij}^+ = {}^{D_{ij}}/_{\nu_{f,wall}} \ . \tag{29}$$

The dimensionless temperature is given by

$$T^+ = {}^{T u_\tau \rho_{f,wall} c_{P,f,wall}}/_{q_w} - T_{wall}^{0+} \ , \tag{30}$$

where

$$T_{wall}^{0+} = {}^{T_{wall} u_\tau \rho_{f,wall} c_{P,wall}}/_{q_w} \ , \tag{31}$$

and $q_w = -\left. k_f \partial_\perp T \right|_{wall}$ is the wall heat flux.

The Prandtl number is given by

$$Pr = {}^{c_P \mu_f}/_{k_f} \ . \tag{32}$$

Constant turbulent Prandtl and Schmidt numbers of $Pr_t = 0.85$ and $Sc_t = 0.7$, respectively, were employed.